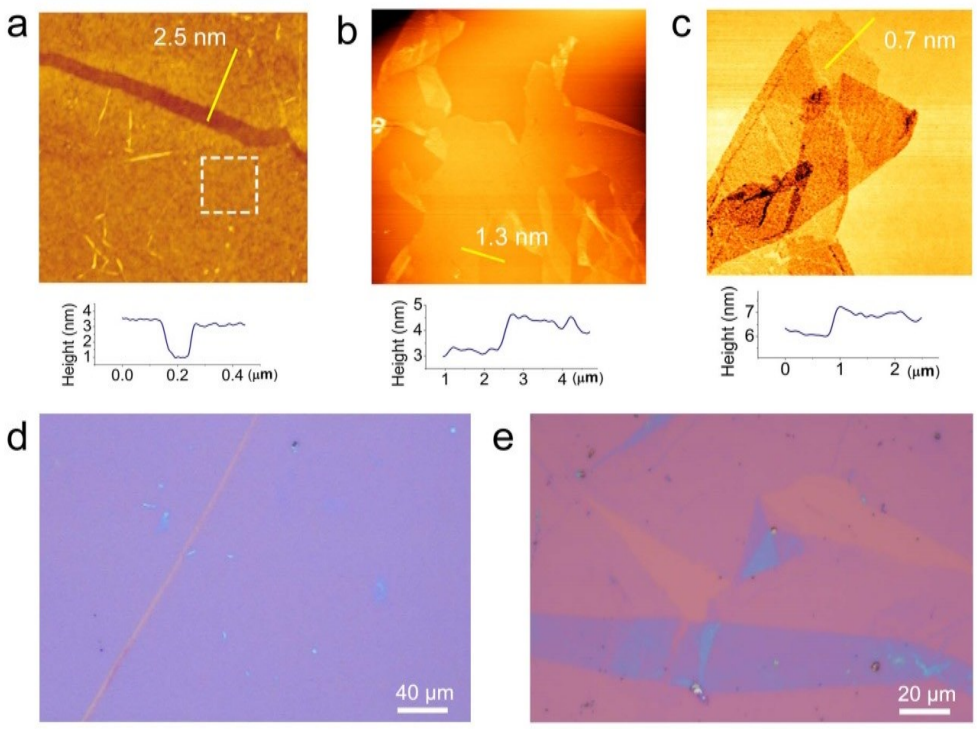


**Supplementary Figure S1. AFM characterizations and topographical defects of h-BN films on silica substrates.** (a) – (c) show the AFM height topographies of h-BN film in a size of ~1.5μm×1.5μm, 30μm×30μm and 10μm×10μm, respectively. Height profiles below showing thicknesses of ~ 0.7, 1.3 and 2.0 nm (corresponding to layer numbers 5~6, 3~4 and 2), respectively. The roughness of the thin layer h-BN can be down to ~300 pm (dashed region in Fig. S1a), comparable to the value of $SiO_2$ (~250 pm).[1] (d) Optical image of ~5nm h-BN on silica. Thick h-BN films can be easily transferred from Cu/Ni foil to other substrates without creating many topographical defects (cracks, pinholes). The purple line was scratched by tweezers showing the color of substrates. (e) PMMA-assisted transfer process introduces a few cracks in double-layered h-BN.

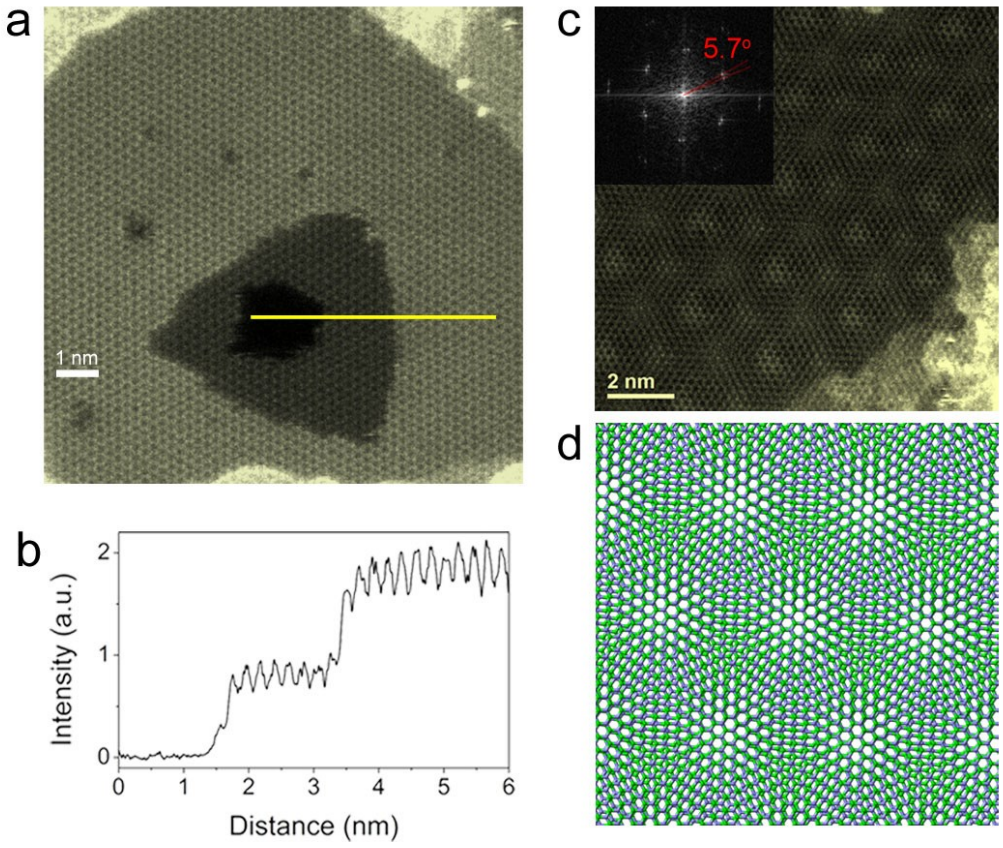


**Supplementary Figure S2. SETM-ADF image of tri-layered h-BN. (a) and (b)** ADF image intensity analysis of h-BN layers. Intensity line profile taken from the highlighted trajectory showing quantized intensity from monolayer and bilayer h-BN. **(c)** Image intensity analysis shows that this region contains three layers of h-BN. FFT of the image suggests that two of the layers have AB stacking without rotation, and the third layer has a ~5.7˚ rotation with respect to the other two layers. Inset is the diffraction pattern of the film showing a rotation angle of 5.7°. **(d)** An illustration of h-BN layers with the same rotation angle between two layers. The green atoms are nitrogen while boron atoms are in purple.

Most of double-layered h-BN is AB stacking. However, for some tri-layered and several layered h-BN we noticed a slight rotation angles among layers, as shown in Supplementary Fig. S2a. Image intensity analysis shows that this region contains three layers of h-BN. FFT of the image suggests that two of the layers have AB stacking without rotation, and the third layer has a ~5.7˚ rotation with respect to the other two layers.

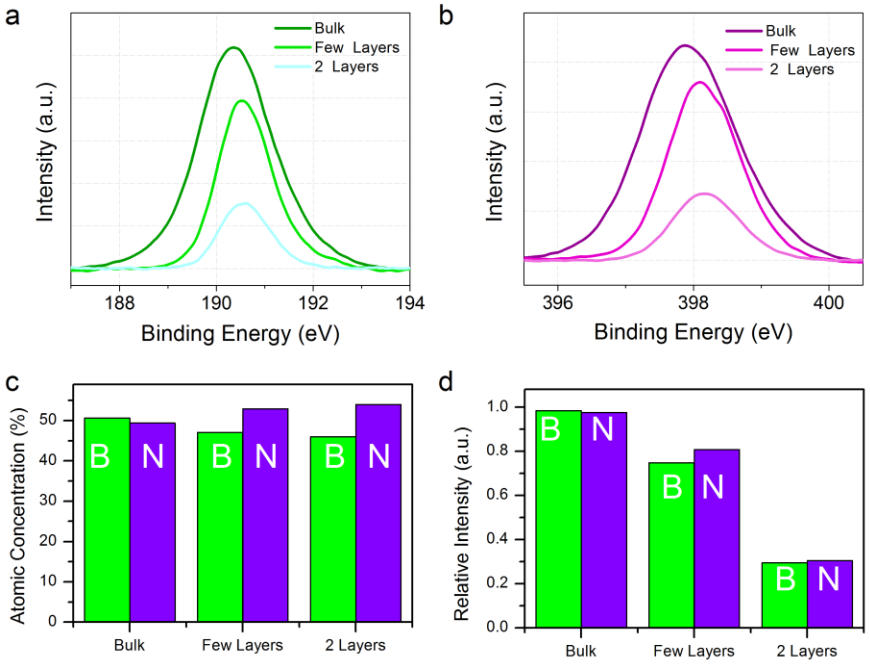


**Supplementary Figure S3. XPS signature of h-BN films.** (a) and (b) XPS spectra of B and N 1s core level of samples in various thickness. (c) and (d) Atomic concentration and relative intensity of B and N.

The XPS spectra of h-BN films with various thicknesses are represented in Supplementary Fig. S3a,b. It is previously reported that the B 1s core level of hexagonal boron nitride locates at ~190 eV and N 1s core level at 398 eV. For the double-layered and few-layered h-BN grown, the peak from B located 190.3 to 190.7 eV, and peak from N locate from 379.9 to 398.2 eV, consistent to the reported values [20, 35]. The XPS spectra of h-BN powder are used for comparison. The B and N peak position are ~ 190.3 and 397.9 eV, close to the value from CVD growth. The atomic concentration of h-BN grown is 50%±4%, showing a good stoichiometry ratio of B and N (Supplementary Fig. S3c). The slighter redundant may come from the nitric residual during transfer. Also, under the same condition, the intensity of h-BN becomes weak while the h-BN film is thinner (Supplementary Fig. S3d).

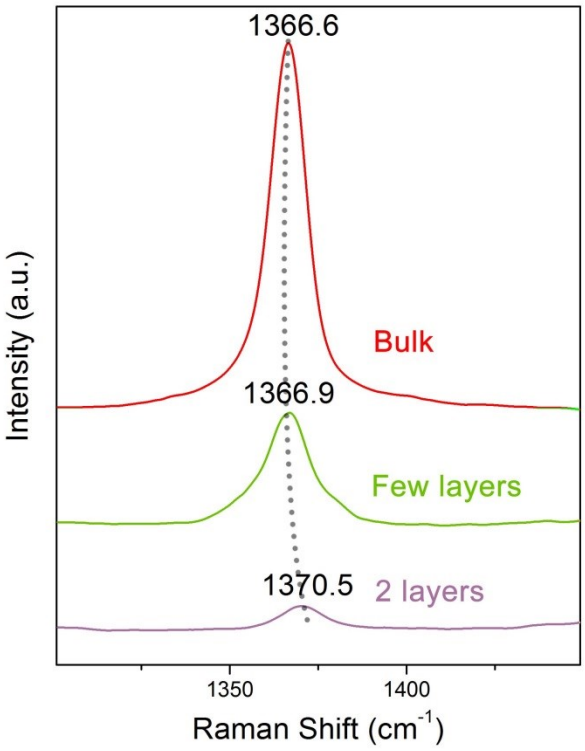


**Supplementary Figure S4.** Raman spectra of double layered, ~ 10 layered and bulk h-BN on $SiO_2$.

The Raman vibration mode of h-BN ($E_{2g}$) was examined [36, 37]. From bulk to double layered h-BN films, the $E_{2g}$ peak shifts from ~1367 $cm^{-1}$ to ~1371 $cm^{-1}$, along with a dramatic drop in Raman intensity (Supplementary Fig. S4). These results agree well with previous report on the Raman signature of mechanical exfoliated h-BN films [20]. Furthermore, the half width at half-maximum (FWHM) of $E_{2g}$ peaks were analyzed to evaluate the quality of h-BN films. For most of h-BN samples grown on Ni foil, the FWHM are ~ 11 $cm^{-1}$, comparable to the value of mechanical exfoliated h-BN (10 ~ 12 $cm^{-1}$). As a comparison, the FWHM of $E_{2g}$ peak from h-BN on Cu substrate is ~16 $cm^{-1}$, suggesting Ni is a much better substrate than Cu for growing high quality h-BN layers.

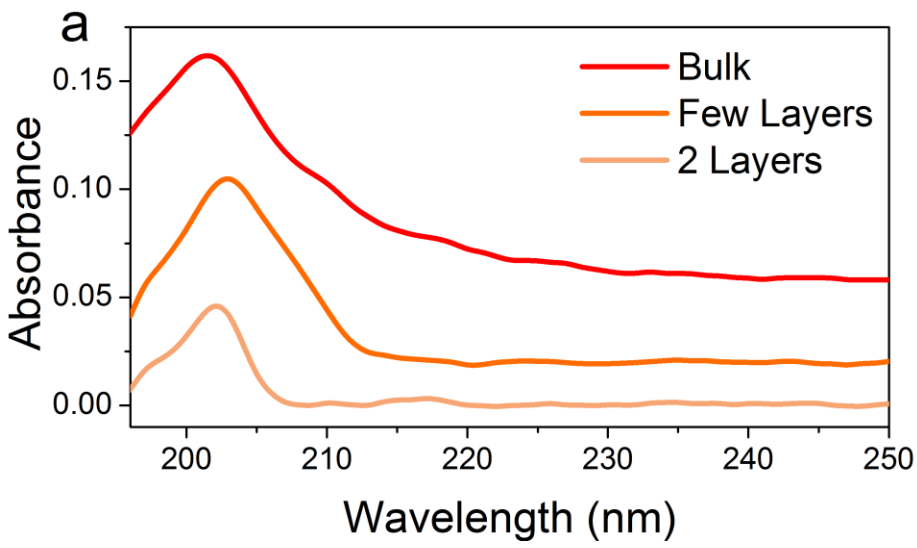


**Supplementary Figure S5. UV adsorption spectra of h-BN layers.**

The h-BN samples (~1 cm × 1 cm) were transferred to quartz substrates. Before measurements, a blank quartz plate was used to determine the baseline of spectra. The transmittance of double-layered, few-layered and several-layered h-BN (~20 nm) are ~99.5%, 98.0%, and 94.0% (Supplementary Fig. S5), higher than ideal transmittance of sing-layered graphene (~97.7%) [7], in the wavelength range of 250 nm ~ 900 nm. All the spectra show only one dominant peak at ~ 202 nm, revealing the low impurity content of our h-BN samples. The corresponding full width at half maximum (FWHM) are ~ 5.3 (double layers), 8.8 (few layers) and 15.8 nm (several layers), which indicates the thin h-BN films may be a better deep ultraviolet light-emitting source [38, 39] because of its narrow spectral bandwidth.

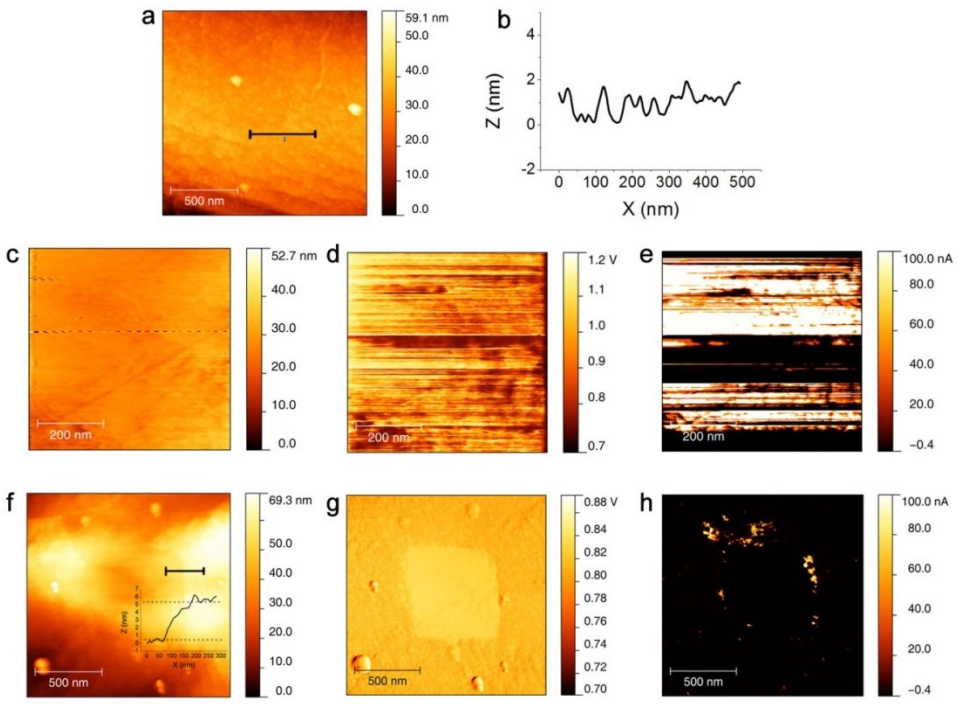


**Supplementary Figure S6. AFM imaging of 5 nm h-BN on Ni foil.** (a) Morphologies of 5nm h-BN on Ni foils. (b) Corresponding height topography. (c) – (d) Topography, friction and current sensing imaging during the AFM lithography, respectively. (f) – (h) Topography, friction and current sensing imaging after the AFM lithography at the same location.

AFM based lithography and imaging were employed to characterize the 5nm coated Ni foils. Supplementary Fig. S6a and S6b show the surface morphologies of the sample. The surface is fully covered by the as-grown h-BN film. To determine the thickness of h-BN films, the h-BN film is etched locally by an AFM tip in contact mode with a high force, as shown in Supplementary Fig. S6c-e (height, friction and current sensing imaging, respectively). A size of ~ 600 nm × 600 nm was etched by the tip. Current signal was observed when the tip is approaching the Ni surface. Supplementary Fig. S6f-h showing the height, friction and current sensing imaging of the same location after AFM lithography. According to Supplementary Fig. S6f, the thickness of h-BN is ~5 nm. Friction imaging represents the difference between Ni furnace (center) and h-BN films. Only weak current signal is obtained because the conductive coatings have been worn out during lithography.

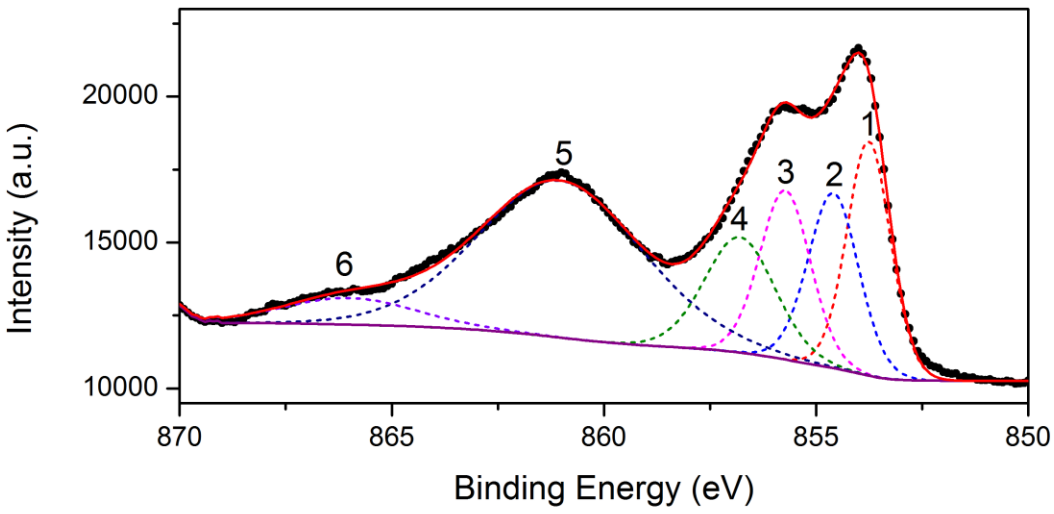


**Supplementary Figure S7. XPS spectrum fitting of the oxidized Ni foil under 1100°C for 30 min.** This spectrum is fitted based on the Ni(II)/Ni(III) multiple structure allowing variation of the multiple spacing and FWHM. Gaussian (70%) - Lorentzian (30%) profiles are chosen for each component. Black dots show the raw data and red line is the sum of all the components. The spectrum shape is very like to the Ni 2p3/2 spectrum of polycrystalline Nickel oxides powder. Label 1-4 are the multiple contributions to the main peak which are often observed in the Nickel oxides. There are also two broad peaks (Label 5 and 6) at a higher banding energy. Peak 5 ( a peak near 7.0 eV) is assigned to a Ni 3d to Ni 4p transition in surface atoms by Hagelin-Weaver et al, while Peak 6 corresponds to the inter-band losses. Such satellite structure is also observed in Fe and Cr 2p spectra.

The fitting parameters please see Supplementary Table S2.

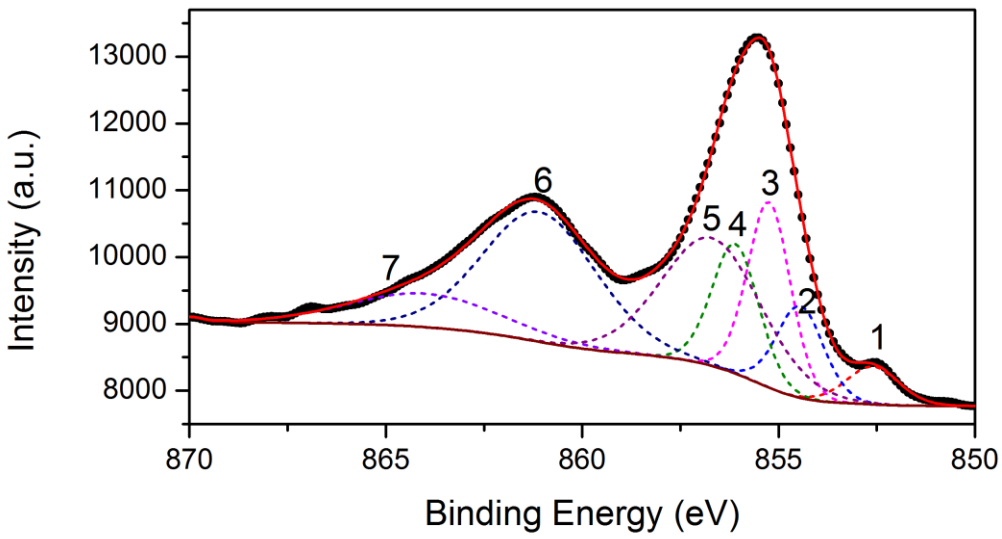


**Supplementary Figure S8. XPS spectrum of the Ni foil with the deposition of 2nm h-BN deposition after oxidation under 1100$^{o}$C.** This spectrum is fitted by dashed lines. Black dots show the raw data and red line is the sum of all the components. Gaussian (70%) - Lorentzian (30%) profiles are chosen for each component. The main peak is consisted of four components. The satellite is also observed. A weak peak from pure Nickel is observed located at ~ 852.6 eV.

The fitting parameters please see Supplementary Table S3.

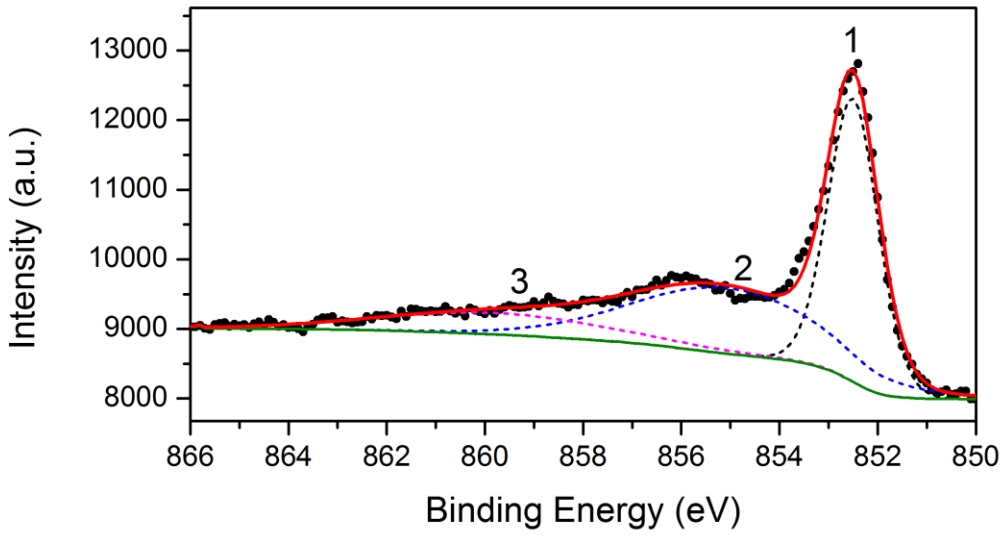


**Supplementary Figure S9. XPS spectrum of the Ni foil with the deposition of 5 nm h-BN deposition after oxidation under 1100$^{o}$C for half an hour.** This is a typical spectrum from Ni 2p, and is fitted by dashed lines. Black dots show the raw data and red line is the sum of all the components. Gaussian (70%) - Lorentzian (30%) profiles are chosen for each component. The main peak is located at ~ 852.5 eV. Two obvious satellites are fitted by board peaks with binding energy near 2.6 eV and 7.3 eV, respectively, due to the possible surface plasmon loss. No nickel oxides signal is found from the spectra (including the depth profile process), suggesting the Ni surface is be well protected from oxidation by depositing 5 nm h-BN film on its surface.

The fitting parameters please see Supplementary Table S4.

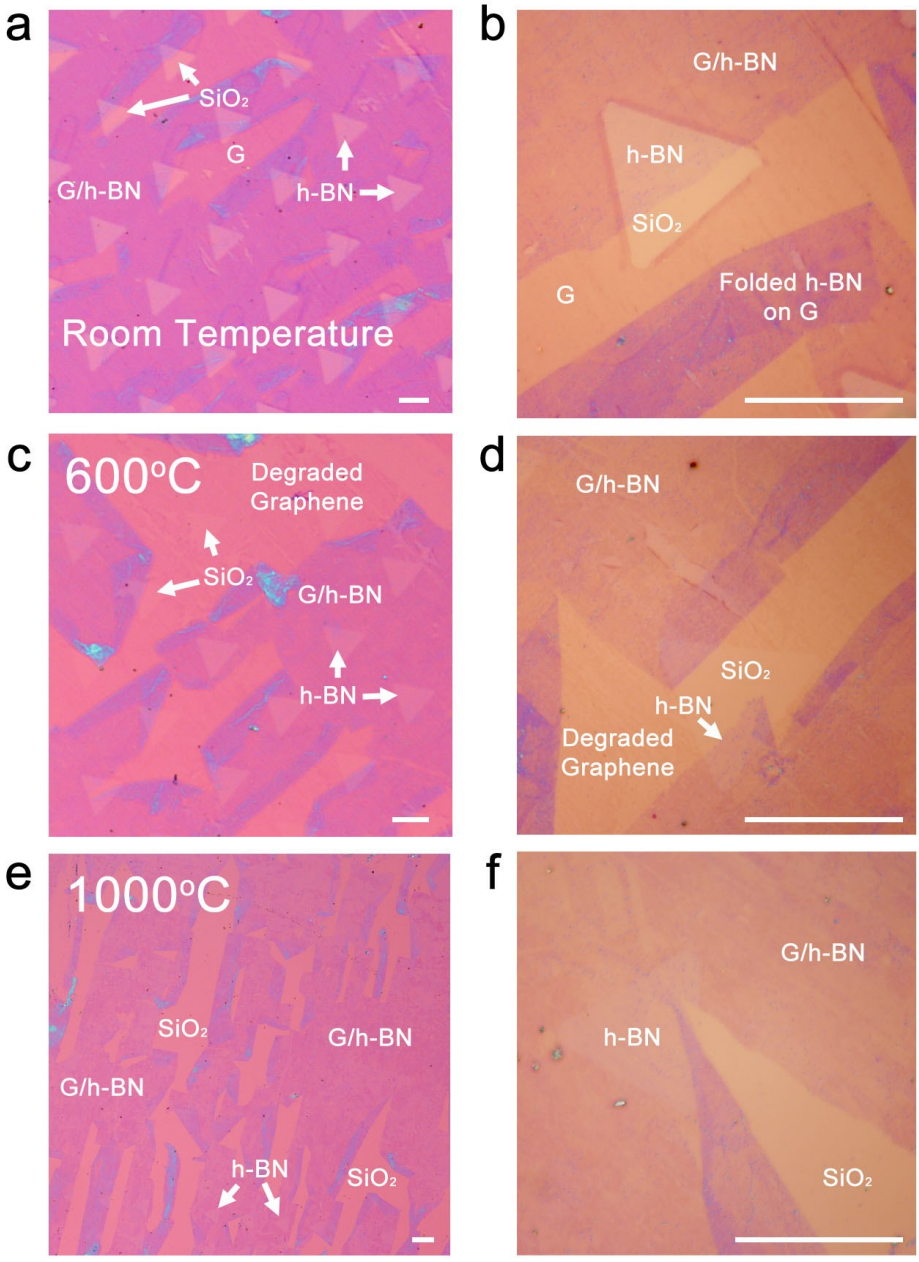


**Supplementary Figure S10. Optical images of 2 nm h-BN coated graphene.** (a) and (b) Morphologies of G/h-BN films at room temperature on the silica substrate. Graphene have been pre-patterned and then transfer h-BN on it. h-BN layers are partially broken or folded during the transfer process. (c) and (d) G/h-BN films after oxidation at 600 $^{o}$C. The contrast of uncovered graphene is much lower than pristine graphene because of degradation, while h-BN films keep the same contrast. (e) and (f) G/h-BN films after oxidation at 1000 $^{o}$C. No graphene can be found at the uncovered regions. However, graphene is still survived at the locations covered by h-BN layers. The thickness of h-BN is ~ 2 nm. Scale bars are 40 μm for all images.

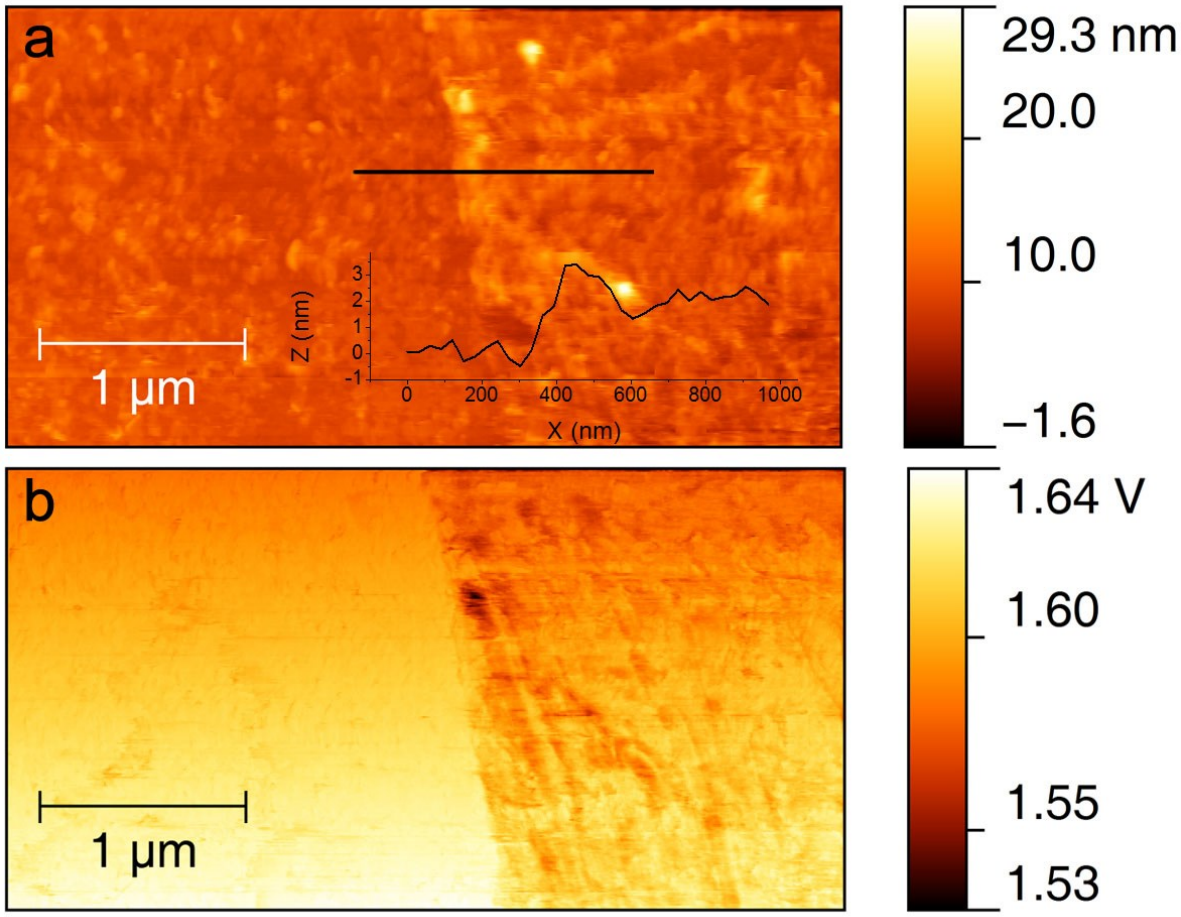


**Supplementary Figure S11. AFM imaging of h-BN coated graphene.** (a) Height imaging. Left region is pure graphene. Right part is h-BN coated graphene. The thickness of h-BN is ~ 2 nm, as shown in the height topography. (b) Friction imaging showing a clear interface between graphene and G/h-BN.

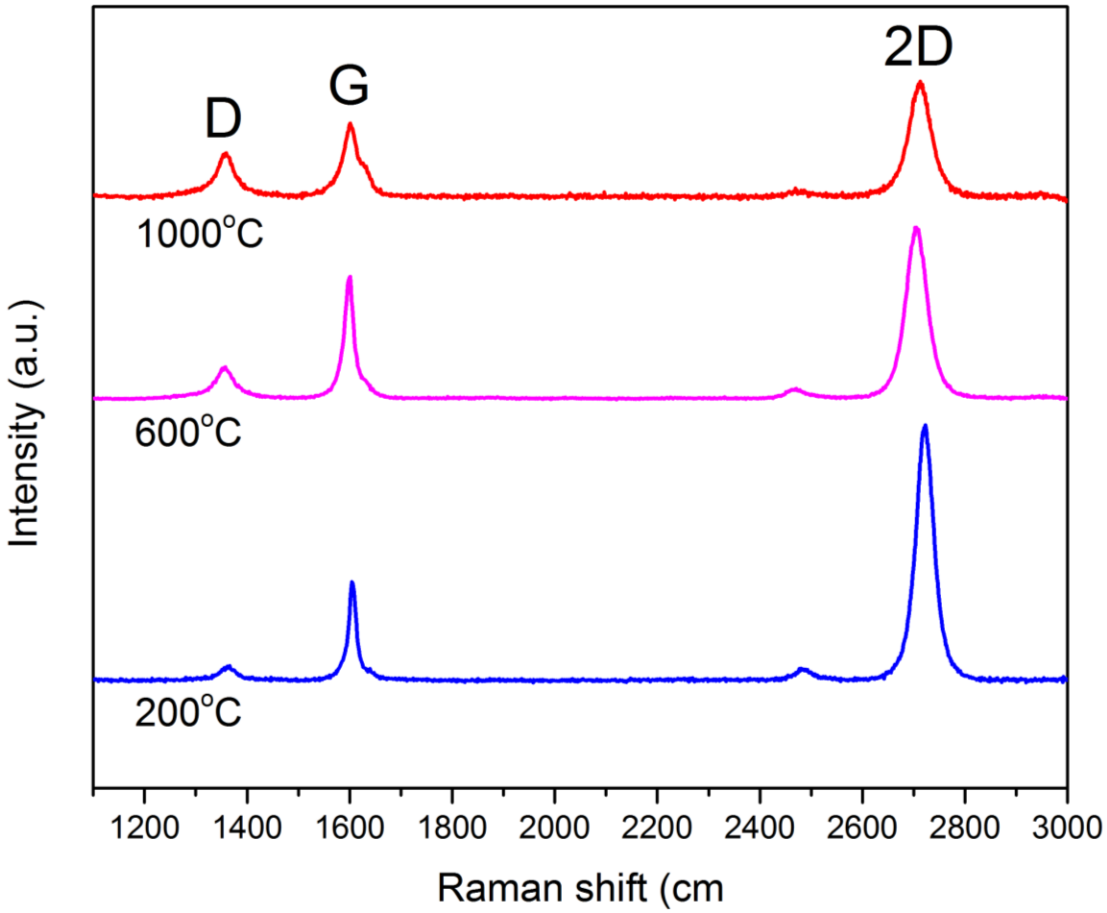


**Supplementary Figure S12. h-BN films as an anti-oxidation coating for graphene on sapphire substrates.** Raman spectra for the h-BN coated graphene on sapphire substrates, under 200 $^{o}$C, 600 $^{o}$C and 1000 $^{o}$C.

**Supplementary Table S1: Growth conditions of h-BN films with various layers on Ni substrates**

| **Thickness of h-BN** | 2 L | Few layers (3 ~10 L) | Several layers (>10 L) |
|---|---|---|---|
| **Growth temperature** | 1000 °C | 1000 °C | 1100 ~ 1200 °C |
| **Growth time** | 1 ~ 1.5 h | 1h | 0.5 h |
| **Precursor temperature** | 40 °C | 50 ~ 70 °C | 70 ~ 90 °C |

**Supplementary Table S2: XPS spectrum fitting parameters for Nis foils oxidized**

| **Peak label** | **Position (eV)** | **FWHM (eV)** | **Area** | **Line Shape** | **% Conc.** |
|---|---|---|---|---|---|
| 1 | 853.76 | 1.202 | 415.6 | GL(30) | 15.661 |
| 2 | 854.59 | 1.4 | 361.2 | GL(30) | 13.61 |
| 3 | 855.73 | 1.4 | 349.2 | GL(30) | 13.159 |
| 4 | 856.8 | 1.953 | 331.7 | GL(30) | 12.501 |
| 5 | 861.03 | 4.561 | 1051.5 | GL(30) | 39.624 |
| 6 | 866 | 3.701 | 144.5 | GL(30) | 5.446 |

**Supplementary Table S3: XPS spectrum fitting parameters for 2 nm h-BN coated Ni foils**

| **Peak label** | **Position (eV)** | **FWHM (eV)** | **Area** | **Line Shape** | **% Conc.** |
|---|---|---|---|---|---|
| 1 | 852.61 | 1.574 | 38.3 | GL(30) | 3.758 |
| 2 | 854.45 | 1.4 | 82.9 | GL(30) | 8.138 |
| 3 | 855.24 | 1.282 | 153.3 | GL(30) | 15.051 |
| 4 | 856.1 | 1.4 | 116.8 | GL(30) | 11.463 |
| 5 | 861.1 | 3.405 | 283.9 | GL(30) | 27.869 |
| 6 | 864 | 4.503 | 96.9 | GL(30) | 9.513 |
| 7 | 856.7 | 3 | 246.6 | GL(30) | 24.208 |

**Supplementary Table S4: XPS spectrum fitting parameters for 5 nm h-BN coated Ni foils**

| **Peak label** | **Position (eV)** | **FWHM (eV)** | **Area** | **Line Shape** | **% Conc.** |
|---|---|---|---|---|---|
| 1 | 852.50 | 1.203 | 210.4 | GL(30) | 44.761 |
| 2 | 855.07 | 4.598 | 186.0 | GL(30) | 39.567 |
| 3 | 859.79 | 5.571 | 73.7 | GL(30) | 15.672 |

## Supplementary References


35. Park, K. S., Lee, D. Y., Kim, K. J. & Moon, D. W. Observation of a hexagonal BN surface layer on the cubic BN film grown by dual ion beam sputter deposition. *Appl. Phys. Lett.* **70**, 315-317 (1997).
36. Blase, X., Rubio, A., Louie, S. G. & Cohen, M. L. Quasiparticle band structure of bulk hexagonal boron nitride and related systems. *Phys. Rev. B* **51**, 6868-6875 (1995).
37. Zunger, A., Katzir, A. & Halperin, A. Optical properties of hexagonal boron nitride. *Phys. Rev. B* **13**, 5560-5573 (1976).
38. Kubota, Y., Watanabe, K., Tsuda, O. & Taniguchi, T. Deep Ultraviolet Light-Emitting Hexagonal Boron Nitride Synthesized at Atmospheric Pressure. *Science* **317**, 932-934 (2007).
39. Li, L. H., Chen, Y., Lin, M.-Y., Glushenkov, A. M., Cheng, B.-M. & Yu, J. Single deep ultraviolet light emission from boron nitride nanotube film. *Appl. Phys. Lett.* **97**, 141104 (2010).